Optica Applicata, Vol. XLVI, No. 4, 2016
DOI: 10.5277/oa160406

Optimal threshold detection for Málaga turbulent optical links

ANTONIO JURADO-NAVAS[1, 2*], JOSÉ MARÍA GARRIDO-BALSELLS[2], MIGUEL CASTILLO-VÁZQUEZ[2], ANTONIO PUERTA-NOTARIO[2], IDELFONSO TAFUR MONROY[1], JUAN JOSÉ VEGAS OLMOS[1]

[1]Department of Photonics Engineering, Technical University of Denmark (DTU), Ørsted Plads, Building 358, 2800 Kgs. Lyngby, Denmark

[2]Department of Communications Engineering, University of Málaga, Campus de Teatinos s/n, 29071 Málaga, Spain

[*]Corresponding author: antnav@fotonik.dtu.dk

A new and generalized statistical model, called Málaga distribution (M distribution), has been derived recently to characterize the irradiance fluctuations of an unbounded optical wave front propagating through a turbulent medium under all irradiance fluctuation conditions. As great advantages associated to that model, we can indicate that it is written in a simple tractable closed -form expression and that it is able to unify most of the proposed statistical models for free-space optical communications derived until now in the scientific literature. Based on that Málaga model, we have analyzed in this paper the role of the detection threshold in a free-space optical system employing an on-off keying modulation technique and involved in different scenarios, and taking into account the extinction ratio associated to the employed laser. First we have derived some analytical expressions for the lower-bound performance of the free-space optical system with the light intensity fading induced by turbulence obtained when the additive white Gaussian noise is not present in the system. Then, we have analyzed the optimal threshold in the system and how it changes when atmospheric conditions vary. Finally, a closed form expression for the bit error rate of that system is derived.

Keywords: atmospheric propagation, atmospheric turbulence, Málaga distribution, scintillation.

1. Introduction

In the last few years, free-space optical (FSO) communication systems are receiving considerable research efforts [1–8] mainly due to their inherent potential transmission capacity, much higher than that offered by radio transmission technologies. Thus, considering their narrow beam widths and their inherent license-free operation as com-

pared with microwave systems, FSO systems are appropriate candidates for secure, high-data-rate, cost-effective, wide-bandwidth communications.

Due to the complexity associated with phase or frequency modulation, current FSO systems typically use intensity modulation with direct detection (IM/DD). However, in those systems, and even in clear sky conditions, FSO links may experience temporal irradiance fluctuations of the received signal intensity (scintillation) associated to the interaction of light with turbulent atmosphere [1]. That scintillation degrades the performance of such links in terms of, for example, an average bit error rate (BER).

This performance is deduced from the probability density function (PDF) of the irradiance. Thus, most widely accepted irradiance PDF models have led to the consideration of conditional random processes [1, 6–8]. In this regard, recently a new and generalized statistical model, called Málaga distribution (M distribution), has been derived and validated [7, 8] to characterize the irradiance fluctuations of an unbounded optical wave front (plane and spherical waves) propagating through a turbulent medium under all irradiance fluctuation conditions in homogeneous, isotropic turbulence. This Málaga distribution unifies most of the irradiance statistical models for FSO communications proposed in literature in a closed-form expression. Its conditional random process is made by a gamma and a compound of the Nakagami-*m* distribution and the Rayleigh random phasor.

In this paper, we perform a study focused on IM/DD optical systems affected by a Málaga statistical model and focused on the effect of the detection threshold for three different scenarios: with complete knowledge about the channel, with partial knowledge or, on the contrary, without it. In all cases, the PDF of the irradiance fluctuation is required to derive subsequent mathematical expressions that support every section in the paper. Hence, after a brief introduction of the Málaga statistical model (Section 2), we introduce the system model considered through this work (Section 3). Then we start studying a system with a fixed detection threshold in Section 4. The type of a system studied in that section is unable to adapt itself to any change in the channel conditions, so a lower bound of working is achieved and perfectly associated to any particular turbulence regime. Thanks to the tractability of the Málaga distribution, we derive the analytical expressions for the lower-bound performance of the FSO system with the light intensity fading induced by turbulence for the widely employed on-off keying (OOK) modulation technique including different pulse shape formats. That lower-bound performance is accomplished when the additive white Gaussian noise is not present in the system. Results provided in Section 4 complete the ones obtained in [9] for both a lognormal and a gamma-gamma turbulence.

Next, Section 5 shows a study of the optimal threshold for a FSO system when the mean and normalized irradiance variances are known. The effect of the laser bias – represented by the extinction ratio – is also considered and its effect is shown in this section. Finally, in Section 6, we detail the analytical expressions for the error probability associated to a system with perfect knowledge of the channel state information (CSI), again including the effect of the extinction ratio in the resulting expressions.

2. Atmospheric channel model

2.1. A previous consideration

Pulses propagating through an atmospheric optical link may be influenced by temporal spreading owing to turbulence, especially in atmospheric areas characterized by sand, and/or dust particles [10, 11]. Normally, these environments may distort the optical pulse shape by means of a temporal broadening since multiple propagation paths can occur when interacting the beam light with the atmospheric particles. Physically, two possible causes exist for this pulse spreading: scattering (dispersion) and pulse wander (fluctuations in arrival time) [11]. If that pulse spreading is present, then its effect is seen as an intersymbol interference (ISI) that should be considered in an analogous manner as multipath effects are incorporated in radiofrequency propagation.

However, as detailed in [10], this temporal broadening is mainly relevant when transmitting very short pulses (with half-widths less than 1 ps) and long distances. For instance, consider a collimated space-time Gaussian beam pulse with an input pulse half-width T_0. After propagating through the atmosphere, its resulting pulse half-width is broadened as [10]

$$T_2 = \sqrt{T_0 + 8\alpha} \tag{1}$$

where α is expressed as

$$\alpha = \frac{0.3908 C_n^2 L L_0^{5/3}}{c^2} \tag{2}$$

and C_n^2 is the atmospheric index of refraction structure parameter, L is the propagation path, L_0 represents the outer scale of the turbulence (we can approximate its value to the height of the transmitter in a terrestrial link), and c is the speed of light. For typical values in the atmospheric link (for instance, $L = 1$ km, $L_0 = 30$ m, and $C_n^2 = 10^{-15}$ m$^{-2/3}$) $\alpha = 1.25 \times 10^{-27}$. Following Eq. (1), the factor 8α becomes equivalent to T_0^2 while T_0 is less than 1 ps. This fact means that to start considering the influence of temporal broadening, we need to transmit data rates above 1 Tb/s. Since typical commercial data rates are around several Gb/s, the effect of temporal broadening and its subsequent ISI is not considered in this paper. Hence, it is assumed that the atmospheric channel has a bandwidth much wider than the one belonging to the transmitted signal.

2.2. Málaga statistical model for the turbulence

Málaga distribution is based on a new small-scale propagation scheme including a new scattering component for the observed field U_S^C coupled to the line-of-sight (LOS) field term U_L. The propagation scheme is illustrated in Fig. 1 [7]. As detailed in [7], the observed field at the receiver is supposed to consist of three terms: the first one is

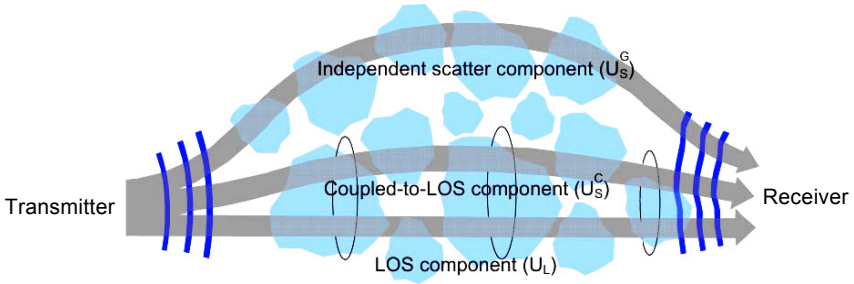

Fig. 1. Proposed propagation geometry for a laser beam in a Málaga model to form the small-scale fluctuations [7].

the LOS contribution U_L, the second one is the component which is quasi-forward scattered by the eddies on the propagation axis U_S^C and coupled to the LOS contribution; whereas the third term U_S^G is due to energy which is scattered to the receiver by off-axis eddies, this latter contribution being statistically independent of the previous two other terms. The inclusion of the coupled to the LOS scattering component U_S^C is the main novelty of the model, as mentioned before, and it can be justified by the high directivity and the narrow beam widths of laser beams in atmospheric optical communications.

Following notation of [7], the average power of the LOS term is represented by Ω while the average power of the total scatter components is denoted by

$$2b_0 = E\left[\left|U_S^C\right|^2 + \left|U_S^G\right|^2\right] \tag{3}$$

with U_S^G being the classic scattering field independent of the LOS contribution. Accordingly, the average power of every single scatter component is given by

$$E\left[\left|U_S^C\right|^2\right] = \rho 2b_0 \tag{4a}$$

and

$$E\left[\left|U_S^G\right|^2\right] = (1-\rho)2b_0 \tag{4b}$$

for the coupled-to-LOS scattering term and for the classic scattering component received by off-axis eddies, respectively. The parameter ρ shows the amount of scattering power coupled to the LOS component, ranging from 0 to 1.

Then, the Málaga PDF of the received irradiance I is represented by:

$$f_I(I) = A\sum_{k=1}^{\beta} a_k I^{\frac{\alpha+k}{2}-1} K_{\alpha-k}\left(2\sqrt{\frac{\alpha\beta I}{\xi_g\beta+\Omega'}}\right) \tag{5a}$$

$$\begin{cases} A = \dfrac{2\alpha^{\alpha/2}}{\xi_g^{1+\alpha/2}\Gamma(\alpha)}\left(\dfrac{\xi_g\beta}{\xi_g\beta+\Omega'}\right)^{\beta+\alpha/2} \\ a_k = \dbinom{\beta-1}{k-1}\dfrac{(\xi_g\beta+\Omega')^{1-k/2}}{(k-1)!}\left(\dfrac{\Omega'}{\xi_g}\right)^{k-1}\left(\dfrac{\alpha}{\beta}\right)^{k/2} \end{cases} \tag{5b}$$

where $\beta \in N$ is the shape parameter of the Nakagami distribution representing the amount of fading factor, with $\Omega' = \Omega + \rho 2b_0$ representing the average power from the coherent contributions, whereas $K_\nu(\cdot)$ is the modified Bessel function of the second kind and order ν. Finally, α is a positive parameter related to the effective number of large-scale cells of the scattering process [6], and arisen from the gamma approximation to a lognormal distribution. In the interest of clarity, the algebraic manipulation to prove this result can be consulted in Appendix A of Ref. [7].

A generalized PDF expression was also obtained in [7, 8] when $\beta \in R$, though the inherent degree of freedom associated to the proposed distribution allows to model almost any behavior with the case of β being a natural number.

3. System model

Consider an IM/DD link using OOK. In these type of systems, and in the absence of turbulence, the electrical current signal induced in the receiver by the action of the received optical wave can be written as

$$i = i_S + i_N \tag{6}$$

after the integration of the received photocurrent for an interval $T_0 \leq T_b$, with T_b being the bit interval of the OOK system [12]. In Eq. (6), i_N represents the shot noise caused by ambient light much stronger than the desired signal and/or by thermal noise in the electronics following the photodetector. Since it is considered as statistically independent of the desired signal i_S, then it is supposed to be modeled as a zero-mean additive white Gaussian noise described by the following PDF:

$$f_n(i) = \frac{1}{\sqrt{2\pi\sigma_N}}\exp\left(-\frac{i^2}{2\sigma_N^2}\right) \tag{7}$$

with σ_N^2 representing the variance of the noise. In addition, $i_S = 2RP_t$ denotes the electrical current associated to the received signal light, with R being the responsivity, whereas P_t is the average of transmitted optical power. Accordingly, the total electrical

current signal induced in the receiver, $i = i_S + i_N$, is also governed by the following non-zero mean Gaussian PDF:

$$f_{s+n}(i) = \frac{1}{\sqrt{2\pi\sigma_N}} \exp\left(-\frac{(i-i_S)^2}{2\sigma_N^2}\right) \tag{8}$$

Thus, we consider an IM/DD link through this paper. The case of an OOK modulation technique is simple since each bit symbol is generated by pulsing the light source either on (logic 1) or off (logic 0) during each bit time. In this respect, errors in the receiver occur when either a 0 is mistaken for a 1, denoted as $P_r(1|0)$ and representing the probability of false alarm; or when a logic 1 is wrong detected as a 0, denoted as $P_r(0|1)$ and expressing the probability of missed detection. These are also called type I and type II errors, respectively [1]. Taking both into account, and following [1], the overall probability of error, $P_r(E)$ is given by the sum of such errors, weighted by the probability of the occurrence of symbols 0 and 1:

$$P_r(E) = p_0 P_r(1|0) + p_1 P_r(0|1) \tag{9}$$

with p_0 representing the transmission probability of a binary 0 whilst p_1 denotes the occurrence probability of a binary 1 symbol, as indicated in [1].

Now, for the realistic case of not having a perfect matched-filter with sufficient bandwidth at the receiver side (for instance, in Fig. 5 employed in [13]), then some ISI may be introduced in the system. There, the cutoff frequencies of both the matched filter and even the inclusion of an optional three-pole Bessel high-pass filter, thought for natural (solar) light suppression, are chosen as a tradeoff that allows us effectively to suppress most of the shot noise power (more intense than the thermal noise power), leading to solely a moderate ISI induced by such filtering. One illustrative example employing the same receiver scheme but for an indoor optical system was studied by the authors in [14]. There, the presence of ISI is responsible for having a worse behavior of 4PPM (pulse position modulation) format with respect to OOK format with duty cycle of 25% when the signaling rate increases (50 to 100 Mb/s) maintaining the bandwidth in the receiver filter.

With such realistic matched filter, a degradation in terms of error probability is suffered by the system in the way derived by KAHN *et al*. (see Eqs. (9) and (10) in [15]) for an IM/DD system with OOK format. Such a conclusion can be directly applied to a FSO communication system, as was demonstrated by AHARONOVICH and ARNON [16]. For that case, the system is first considered without taking into account the effect of turbulent atmosphere, but only the effect of additive white Gaussian noise and ISI. Consequently the BER is expressed according to Eq. (13) in [16] and then, such an expression should be conditioned to the PDF of the irradiance fluctuation to obtain the average BER associated to the system.

Finally, and since we have considered that the atmospheric channel is not introducing any type of temporal broadening (as explained in the previous section), we assume that

it is possible to design an ideal receiver completely adapted to the transmitted signal. We will suppose here that the receiver has a sufficient bandwidth and, consequently, the scope of this paper is focused on how the effect of the atmospheric scintillation is affecting the position of an optimum detection threshold.

4. Analytical expression for the error floor under Málaga turbulence

In [9], the authors developed a procedure to obtain the error floor associated to an atmospheric optical system when the shot noise is completely removed from the system and, consequently, errors are produced uniquely by the presence of scintillation. In this regard, it is assumed that the receiver signal-to-noise ratio (SNR) is limited by shot noise caused by ambient light and modeled following an additive white Gaussian noise of zero mean and variance σ_N^2 that is statistically independent of the desired signal [12]. Accordingly, type I and II errors for a given threshold value in the receiver i_u can be written, from Eqs. (7) and (8), as:

$$P_r(1|0) = \frac{1}{\sqrt{2\pi\sigma_N^2}} \int_{i_u}^{\infty} \exp\left(-\frac{i^2}{2\sigma_N^2}\right) \mathrm{d}i = \frac{1}{2}\operatorname{erfc}\left(\frac{i_u}{\sqrt{2\sigma_N^2}}\right) \tag{10}$$

$$P_r(0|1) = \frac{1}{\sqrt{2\pi\sigma_N^2}} \int_0^{\infty} \left[\int_{-\infty}^{i_u} \exp\left(-\frac{(i-i_S)^2}{2\sigma_N^2}\right) \mathrm{d}i\right] f_I(I)\,\mathrm{d}I \tag{11}$$

In Eqs. (10) and (11), $i_S = 2RI$ is the signal current in the detector induced by the incident optical wave, with R being the responsivity of the photodetector, and with I denoting the received irradiance of the beam. Finally, $f_I(I)$ represents the PDF of the irradiance fluctuations, given by a Málaga distribution in this paper, as was shown in Eq. (5).

Next, as detailed in [9], additive white Gaussian noise is completely removed of from the system when we consider the limit of Eq. (9) when $\sigma_N \to 0$. For this purpose, the definition of the Dirac delta function is considered and identified in Eq. (11), resulting that

$$\lim_{\sigma_N \to 0}[P_r(E)] = p_1 \lim_{\sigma_N \to 0}[P_r(0|1)] = p_1 \int_0^{i_u} f_I\left(\frac{i}{R}\right) \mathrm{d}i \tag{12}$$

Now we can substitute Eq. (5) into Eq. (12):

$$\lim_{\sigma_N \to 0}[P_r(E)] = p_1 A \sum_{k=1}^{\beta} a_k \int_0^{i_u} \left(\frac{i}{R}\right)^{\frac{\alpha+k}{2}-1} K_{\alpha-k}\left(2\sqrt{\frac{\alpha\beta i}{R(\xi_g\beta+\Omega')}}\right) \mathrm{d}i \tag{13}$$

Hence, consider

$$\Im = \int_0^{i_u} \left(\frac{i}{R}\right)^{\frac{\alpha+k}{2}-1} K_{\alpha-k}\left(2\sqrt{\frac{\alpha\beta i}{R(\xi_g\beta+\Omega')}}\right) \mathrm{d}i \tag{14}$$

If we normalize the variable of integration by means of the change of variables: $i = i_u y$ and $\mathrm{d}i = i_u \mathrm{d}y$, then $\Im$ can be written as

$$\Im = i_u \int_0^1 \left(\frac{i_u y}{R}\right)^{\frac{\alpha+k}{2}-1} K_{\alpha-k}\left(2\sqrt{\frac{\alpha\beta i_u y}{R(\xi_g\beta+\Omega')}}\right) \mathrm{d}y \tag{15}$$

and, consequently, it is straightforward to identify Eq. (6.592-2) in [17], given by:

$$\int_0^1 x^{\lambda}(1-x)^{\mu-1} K_{\upsilon}(a\sqrt{x})\mathrm{d}x = \frac{2^{\upsilon-1}}{a^{\upsilon}}\Gamma(\mu) G_{1,3}^{2,1}\left(\frac{a^2}{4}\middle| \begin{matrix} \frac{\upsilon}{2}-\lambda \\ \upsilon, 0, \frac{\upsilon}{2}-\lambda-\mu \end{matrix}\right) \tag{16a}$$

$$\left[\mathrm{Re}(\lambda) > -1 + \frac{1}{2}|\mathrm{Re}(\upsilon)|, \ \mathrm{Re}(\mu) > 0\right] \tag{16b}$$

with $G_{a,\,b}^{c,\,d}(\cdot)$ being the classical Meijer G-function whereas $\Gamma(\cdot)$ represents the gamma function. By applying Eqs. (16) to (15), then Eq. (13) can be solved in a closed-form expression

$$\lim_{\sigma_N \to 0}[P_r(E)] = \frac{p_1 AR}{2}\sum_{k=1}^{\beta} a_k \left(\frac{i_u}{R}\right)^{\frac{\alpha+k}{2}} \frac{G_{1,3}^{2,1}\left(\frac{\alpha\beta i_u}{R(\xi_g\beta+\Omega')}\middle| \begin{matrix} 1-k \\ \alpha-k, 0, -k \end{matrix}\right)}{\left(\sqrt{\frac{\alpha\beta i_u}{R(\xi_g\beta+\Omega')}}\right)^{\alpha-k}} \tag{17}$$

By substituting A and a_k from Eq. (5), and after compacting terms, Eq. (17) is finally written as

$$\lim_{\sigma_N \to 0}[P_r(E)] = p_1(\xi_g\beta+\Omega')^{1-\beta}\frac{(\xi_g\beta)^{\beta}}{\Gamma(\alpha)}\sum_{k=1}^{\beta} R^{-k}(\xi_g\beta+\Omega')^{-k/2}\left(\frac{\alpha i_u}{\xi_g}\right)^k \times$$
$$\times \frac{(\Omega')^{k-1}}{(k-1)!}\binom{\beta-1}{k-1} G_{1,3}^{2,1}\left(\frac{\alpha\beta i_u}{R(\xi_g\beta+\Omega')}\middle| \begin{matrix} 1-k \\ \alpha-k, 0, -k \end{matrix}\right) \tag{18}$$

Now, if we consider the expression of the second moment of the Málaga probability distribution, $m_2(I)$ (see Eq. (26) in [7]), and after some analytical manipulations, we can write Eq. (18) as

$$\lim_{\sigma_N \to 0} [P_r(E)] = p_1 \frac{1}{[\beta \Gamma(\alpha+2)]^2} \sum_{k=1}^{\beta} \Xi(k) (\xi_g \beta + \Omega')^{-2-\frac{k}{2}} \times$$

$$\times \left(\frac{\alpha i_u}{R\beta}\right)^k G_{1,3}^{2,1}\left(\frac{\alpha\beta i_u}{R(\xi_g\beta+\Omega')} \middle| \begin{matrix} 1-k \\ \alpha-k,\, 0,\, -k \end{matrix} \right) \tag{19}$$

where we have identified the second moment of the Málaga probability distribution as $m_2(I) = \sum_{k=1}^{\beta} \Xi(k)$. Hence, it is straightforward to observe that the previous error floor is only depending on the intensity of the turbulence $\sigma_I^2 \approx [m_2(I) - 1]$, and on the magnitude of the threshold itself i_u. Accordingly, if we assume both $R = 1$ and $i_u = I_0/2$, with I_0 being the level of the transmitted irradiance in the absence of air turbulence, we can obtain the minimum error probabilities when the shot noise is completely removed from the system. They are indicated in Table 1 for different values of the Málaga turbulence.

Minimum error floors included in Table 1 were corroborated by a Monte Carlo simulation for an IM/DD atmospheric link affected by Málaga turbulence and identical conditions as the ones shown in Table 1. Those simulated results are displayed in Fig. 2, where the detection threshold was established to $i_u = I_0/2$. The simulation was performed by using a non-return to zero (NRZ) modulation technique following an OOK format. In addition, we have also included the behavior associated to Gaussian pulse shapes (OOK-GS) [3] with different duty cycle, following the criterion of limited average optical power so that the signal amplitude can be increased as the duty cycle is decreased in order to maintain constant the average optical power. Accordingly, as discussed in [3], the peak-to-average optical power ratio (PAOPR) increases and, consequently, a better performance in terms of a BER can be expected. Hence, as can be observed, the use of distinct pulse shapes (Gaussian instead of NRZ) and the utilization of different duty

T a b l e 1. Error floor for OOK and gamma-gamma atmospheric channel.

$\lim[P_r(E)]$	α	β	Ω	ρ	σ_I^2
2.778×10^{-1}	1	1	0.8333	0.82	3.00
2.023×10^{-1}	4	3	0.39	0.33	1.21
1.586×10^{-1}	8	2	0.87	0.89	0.70
8.80×10^{-2}	10	5	0.99	0.75	0.32
4.76×10^{-2}	11	10	0.9999	0.9999	0.20
3.80×10^{-3}	200	20	0.95	0.94	0.061

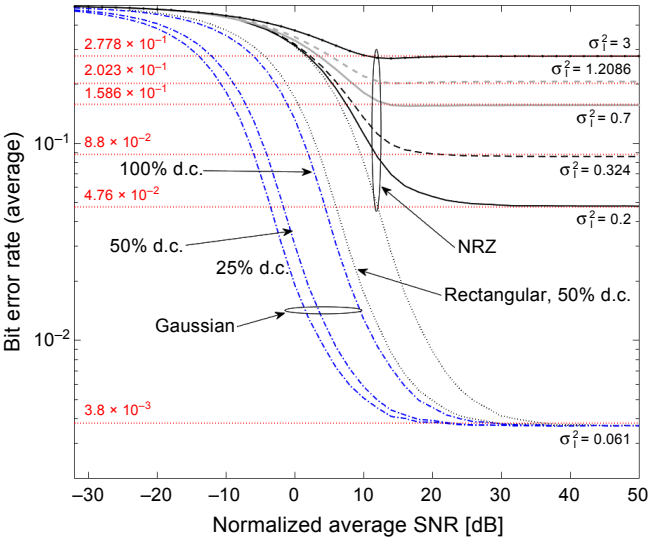

Fig. 2. BER performance and error floor associated to an optical communication system employing OOK-GS and rectangular pulse shapes with different duty cycle (d.c.) and affected by Málaga turbulence. In red dotted line, the error floor values obtained from Eq. (19) and shown in Table 1.

cycles in the pulse, less than 100%, have no influence on the resulting error floor. Certainly, the OOK-GS format initially presents a better performance than a rectangular NRZ pulse shape for lower signal-to noise ratios as a direct consequence of having a higher PAOPR. However, both pulse shapes tend to the same value of the error floor for any concrete intensity turbulence, σ_I^2 and the same threshold detection i_u. The same conclusion is appreciated when different duty cycles are employed; thus if the resulting pulse format is affected by the same turbulence regime, then the error floor associated to the optical system is placed at the same value, as corroborated in Fig. 2.

5. Adaptive system with optimized detection threshold

The error floor shown in Fig. 2 was obtained when the threshold detection value was fixed to $i_u = I_0/2$, regardless of the conditions of the link. Now, in this section, we show the formalisms corresponding to optimal threshold values without requiring a perfect knowledge of the instantaneous channel state information (CSI), although the turbulence PDF and its mean value and variance will be supposed to be known. This fact will reduce the expected computational load of the receiver at high data rates when scintillation can be considered as a stationary random process in a first approximation.

That latter assumption means that all statistics associated to a random process (turbulence, in this case) will solely depend on time differences and not on the specific time origin. Nevertheless, and from a practical point of view, here the weakest condition of a stationary process in the wide sense is only required, which demands only that both the mean value and the covariance be invariant under displacements in time,

i.e., the assumption of isotropy is supposed in this section. More specifically, we consider that the turbulence is not a stationary process but has stationary increments. We can take advantage of this feature since the turbulent process is considered slow, *i.e.*, it will not change significantly during a finite observation time. In addition, it is perfectly valid to assume that the receiver can know the mean μ_I and the variance σ_I^2 of the received irradiance fluctuations after being affected by the turbulence. A plausible reason to justify that point is that the information can be available by using a pilot symbol every interval of 1–10 ms, depending on the coherence time associated to the turbulent process [18].

5.1. Ideal case

Consider the model depicted in Section 3. Assume that the desired signal i_S associated to the transmission of a logic 1 can be written as

$$i_S = k i_u, \qquad k \in [1, \infty) \tag{20}$$

with i_u denoting the detection threshold, and k being a positive parameter. In the absence of turbulence, we can write the probability of false alarm and the probability of missed detection, respectively, as

$$P_r(1|0) = \frac{1}{\sqrt{2\pi\sigma_N^2}} \int_{i_u}^{\infty} \exp\left(-\frac{i^2}{2\sigma_N^2}\right) \mathrm{d}i = \frac{1}{2}\operatorname{erfc}\left(\frac{i_S}{k\sqrt{2\sigma_N^2}}\right) \tag{21}$$

$$P_r(0|1) = \frac{1}{\sqrt{2\pi\sigma_N^2}} \int_{-\infty}^{i_u} \exp\left(-\frac{(i-i_S)^2}{2\sigma_N^2}\right) \mathrm{d}i = \frac{1}{2}\operatorname{erfc}\left(\frac{i_S(k-1)}{k\sqrt{2\sigma_N^2}}\right) \tag{22}$$

Nevertheless, in the presence of atmospheric optical turbulence, the probability of error written in Eq. (22) is considered as a conditional probability that must be averaged over the PDF of the irradiance fluctuation $f_I(h)$ given in Eq. (5), whilst it is assumed that scintillation does not affect the transmission of symbol logic 0 [19]. Thus:

$$\langle P_r(1|0)\rangle = \frac{1}{2}\operatorname{erfc}\left(\frac{\langle i_S\rangle}{k\sqrt{2\sigma_N^2}}\right) \tag{23}$$

$$\langle P_r(0|1)\rangle = \frac{1}{2}\int_0^{\infty} \operatorname{erfc}\left(\frac{\langle i_S\rangle(kh-1)}{k\sqrt{2\sigma_N^2}}\right) f_I(h)\mathrm{d}h \tag{24}$$

where $\langle i_S\rangle = 2RP_t$, as defined in Section 3. To numerically evaluate the integral in Eq. (24), we will assume that the PDF model for irradiance fluctuations is, again, the Málaga distribution shown in Eq. (5).

If CSI is not available then we can take advantage of the fact that scintillation can be considered as a slow process compared to large data rates typical of optical transmission. Consequently, we can use some pilot signals to determine the corresponding mean and variance values associated to scintillation. Then, the need to compute the maximum likelihood (ML) function for any received symbol can be avoided. After analyzing each pilot signal, the decision threshold can be adaptively updated. This is preferred instead of using a static threshold as the one implemented in Section 4, which was demonstrated to be inefficient since it induces a rapid error floor. Then, as a decision metric, we can calculate the likelihood function as

$$\Delta(i_u) = \frac{\langle P_r(0|1)\rangle}{\langle P_r(1|0)\rangle} = 1 \tag{25}$$

as indicated in [12, 19]. Then substituting Eqs. (23) and (24) in Eq. (25), and utilizing a root-finding method, we can obtain the value of k and, accordingly, the different threshold values adapted to each intensity of turbulence monitored by the pilot symbol, considering from Eq. (20) that

$$i_u = \frac{2RP_t}{k}, \qquad k \in [1, \infty) \tag{26}$$

5.2. Case with non-ideal extinction ratio

Real lasers employed in optical communication systems do not present an ideal behavior. On the contrary, they operate with finite power levels for the low and high states and thus, the transmission of a logic 0 is associated to a level of power higher than zero. Consider that instantaneous optical power $s(t)$ in an OOK IM/DD system, can be expressed as

$$s(t) = \sum_k a_k P_{\text{peak}} p_n(t - kT_b) + \zeta \tag{27}$$

where a_k is the random variable with values of 0 for the logic bit 0 (off pulse) and 1 for the bit 1 (on pulse), respectively; P_{peak} is the pulse peak power, whereas $p_n(t)$ is the pulse shape with normalized peak power with $p_n(t) = 1$ for $0 < t < T_b$, with T_b being the bit period. For simplicity, consider that $P_{\text{peak}} = 1$ unless it is said differently. Thus we can assume that the electrical currents corresponding to the received signal light associated to the transmission of a logic 0, i_{S_0}, and to a logic 1, i_{S_1}, are represented by

$$i_{S_0} = \zeta i_S \tag{28a}$$

$$i_{S_1} = i_S + \zeta i_S = i_S(1 + \zeta) \tag{28b}$$

with ζ being a positive parameter that indicates a non-ideal laser transmitting an amount of power for the 0 logic state, *i.e.*, operating with an extinction ratio given by the ratio

$(1 + \zeta)/\zeta$. Therefore, this latter represents how efficiently the power supplied by any available laser transmitter is converted to modulation power. Finally, i_S represents the mean value of the current associated to the received signal light in the ideal case of the absence of turbulence and infinite extinction ratio, *i.e.*, $i_S = 2RP_t$, as indicated in previous sections.

Consider, again, the relationship shown in Eq. (20). Then, for the ideal case of the absence of turbulence, the probability of a false alarm and the probability of a missed detection are now written in the following manner:

$$P_r(1|0) = \frac{1}{\sqrt{2\pi\sigma_N^2}} \int_{i_u}^{\infty} \exp\left(-\frac{(i - i_{S_0})^2}{2\sigma_N^2}\right) \mathrm{d}i = \frac{1}{2}\operatorname{erfc}\left(\frac{i_S(1 - k\zeta)}{k\sqrt{2\sigma_N^2}}\right) \tag{29}$$

$$P_r(0|1) = \frac{1}{\sqrt{2\pi\sigma_N^2}} \int_{-\infty}^{i_u} \exp\left(-\frac{(i - i_{S_1})^2}{2\sigma_N^2}\right) \mathrm{d}i = \frac{1}{2}\operatorname{erfc}\left(\frac{i_S[k(1 + \zeta) - 1]}{k\sqrt{2\sigma_N^2}}\right) \tag{30}$$

Now, the effect of the atmospheric turbulence can be included. Then we can average the two previous expressions over the Málaga PDF following a procedure similar to the one explained in the previous section. Hence, we can obtain:

$$\langle P_r(1|0)\rangle = \frac{1}{2}\int_0^{\infty} \operatorname{erfc}\left(\frac{\langle i_S\rangle(1 - k\zeta h)}{k\sqrt{2\sigma_N^2}}\right) f_I(h)\mathrm{d}h \tag{31}$$

$$\langle P_r(0|1)\rangle = \frac{1}{2}\int_0^{\infty} \operatorname{erfc}\left(\frac{\langle i_S\rangle[k(1 + \zeta)h - 1]}{k\sqrt{2\sigma_N^2}}\right) f_I(h)\mathrm{d}h \tag{32}$$

Figure 3 shows some optimal threshold value i_u adapted to several intensities of Málaga turbulence, for the cases of an ideal and non-ideal extinction ratio.

As we can observe in Fig. 3, the threshold value for optimal decision solely requires being adapted to the intensity of turbulence. Thus, as σ_I^2 increases, the optimal detection threshold decreases since the scintillation, seen as a multiplicative fluctuation in the irradiance, increases the fluctuation of the signal level associated to the transmission of a binary logic 1; whilst the fluctuation corresponding to the signal intensity is unchanged in the ideal case of an infinite extinction ratio. For this ideal case, when the additive white Gaussian noise variance increases, the fluctuations associated to both the binary logic 0 and the binary logic 1 become almost identical in the limit. Accordingly, this latter becomes the main source contributing to the intensity fluctuation in the signal transmitted, much higher than the one associated to the turbulence -induced scintillation. For that reason, the threshold value tends to 0.5 ($k = 2$), as it is shown in Fig. 3.

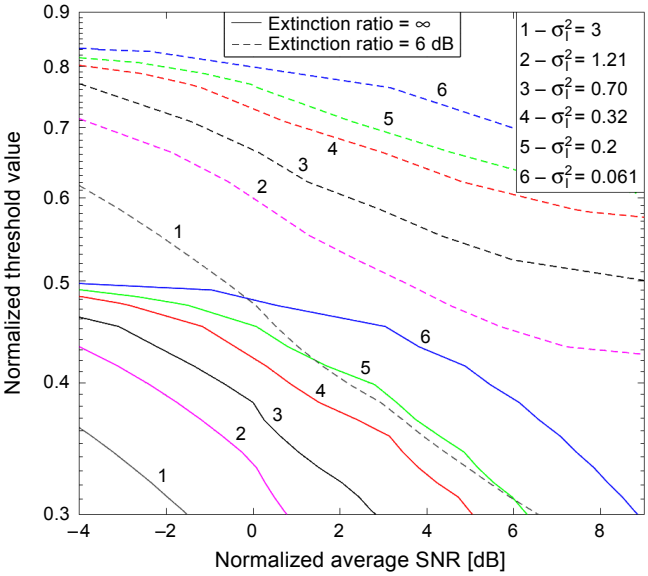

Fig. 3. Optimal threshold value i_u adapted to different intensities of Málaga turbulence, for the cases of ideal and non-ideal extinction ratio. Turbulent channel parameters (α, β, Ω, ρ) were taken from Table 1.

For the case of non-ideal extinction ratio with a value of, *e.g.*, 6 dB ($\zeta = 0.3354$), conclusions are similar, but the upper limit tends to 0.8354 ($k = 1.197$). For the generic case of $\zeta > 0$, the upper limit tends to $0.5 + \zeta$.

On the other hand, when turbulence-induced fading is weaker, then the additive white Gaussian noise is the dominant source of error. For that reason, optimum thresholds are placed in higher values – near the mean value associated to a binary logic 1 – to avoid non-desired threshold crossings induced by the additive white Gaussian noise.

As turbulence is considered a slow process, compared to the large data rates typical of optical transmissions, the system can adapt its threshold detection depending on the mean and variance values associated to the fluctuating received intensity signal and monitored by a pilot signal.

6. Bit error rate with non-ideal extinction ratio

In this section, we will calculate the unconditional average BER of the optical system. Normally, in [1], the ideal probability of error in the absence of turbulence is averaged over the PDF of the irradiance fluctuation so that the CSI is assumed to be known. This latter is considered realistic since, as indicated in previous sections, the turbulence process will not change significantly during a finite observation time. As a direct consequence, it is possible to consider the same state of the channel for several hundreds of thousands of received bits. Then, the implementation of a scheme including the transmission of one pilot symbol every atmospheric coherence time is considered

feasible. To this end, the conditional probabilities obtained in Eqs. (29) and (30) must be averaged over the PDF of the Málaga distribution shown in Eq. (5). By doing that, the BER expression obtained from Eq. (9), and with the help of Eqs. (29) and (30), becomes an average BER:

$$\langle P_r(1|0)\rangle = \frac{1}{2}\int_0^{\infty} \mathrm{erfc}\left(\frac{\langle i_S\rangle(1-k\zeta)h}{k\sqrt{2\sigma_N^2}}\right) f_I(h)\mathrm{d}h \tag{33}$$

$$\begin{aligned}\langle P_r(0|1)\rangle &= \frac{1}{2}\int_0^{\infty} \mathrm{erfc}\left(\frac{\langle i_S\rangle[k(1+\zeta)-1]h}{k\sqrt{2\sigma_N^2}}\right) f_I(h)\mathrm{d}h = \\ &= \frac{1}{2}A\sum_{k=1}^{\beta} a_k \int_0^{\infty} h^{\frac{\alpha+k}{2}-1} \mathrm{erfc}\left(\frac{\langle i_S\rangle[k(1+\zeta)-1]h}{k\sqrt{2\sigma_N^2}}\right)\times \\ &\times K_{\alpha-k}\left(2\sqrt{\frac{\alpha\beta h}{\xi_g\beta+\Omega'}}\right)\mathrm{d}h\end{aligned} \tag{34}$$

Equations (33) and (34) can be solved by writing both the erfc(·) and the modified Bessel functions as Meijer *G*-functions by employing Eqs. (07.34.03.0619.01) and (07.34.03.0605.01) [20], respectively. Thus:

$$\begin{aligned}\langle P_r(1|0)\rangle &= \frac{2^{\alpha-1}A}{8\pi\sqrt{\pi}}\left(\frac{\xi_g\beta+\Omega'}{\alpha\beta}\right)^{\alpha/2}\sum_{k=1}^{\beta}2^k\left(\frac{\xi_g\beta+\Omega'}{\alpha\beta}\right)^{k/2}a_k\times \\ &\times G_{5,2}^{2,4}\left(\frac{32R^2P_t^2(1-\zeta k)^2}{k^2\sigma_N^2}\left(\frac{\xi_g\beta+\Omega'}{\alpha\beta}\right)^2\middle|\begin{matrix}\frac{1-\alpha}{2},\frac{2-\alpha}{2},\frac{1-k}{2},\frac{2-k}{2},1\\ 0,\frac{1}{2}\end{matrix}\right)\end{aligned} \tag{35}$$

$$\begin{aligned}\langle P_r(0|1)\rangle &= \frac{2^{\alpha-1}A}{8\pi\sqrt{\pi}}\left(\frac{\xi_g\beta+\Omega'}{\alpha\beta}\right)^{\alpha/2}\sum_{k=1}^{\beta}2^k\left(\frac{\xi_g\beta+\Omega'}{\alpha\beta}\right)^{k/2}a_k\times \\ &\times G_{5,2}^{2,4}\left(\frac{32R^2P_t^2[k(1+\zeta)-1]^2}{k^2\sigma_N^2}\left(\frac{\xi_g\beta+\Omega'}{\alpha\beta}\right)^2\middle|\begin{matrix}\frac{1-\alpha}{2},\frac{2-\alpha}{2},\frac{1-k}{2},\frac{2-k}{2},1\\ 0,\frac{1}{2}\end{matrix}\right)\end{aligned} \tag{36}$$

where the Meijer *G*-function can be numerically evaluated in a straightforward manner with the aid of the algorithm (presented in Table II [21]). Both equations can be now

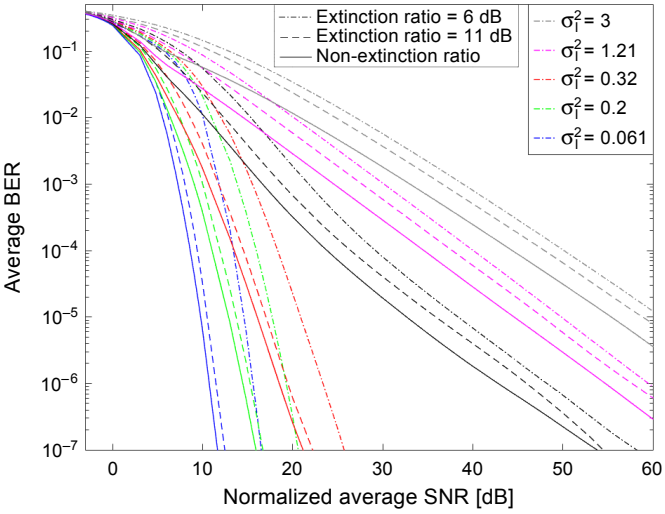

Fig. 4. Average BER *vs.* normalized SNR for different values of extinction ratio. The threshold detection was fixed to $i_u = \langle i_S \rangle/2$.

included in Eq. (9) to obtain a closed-form expression for the average BER associated to an IM/DD atmospheric optical system with an non-ideal extinction ratio. Obtained results were shown in Fig. 4. There we have displayed the behavior of the system for different turbulence intensities, assuming that the occurrence probabilities are $p_0 = p_1 = 0.5$, and fixing $k = 2$ for the threshold detection in all cases. Figure 4 highlights an ideal extinction ratio system, which can be equated to a system using an external Mach–Zehnder modulator [22]. Furthermore, two additional systems are shown with an extinction ratio of 11 and a 6 dB, respectively. The first one is aligned with directly modulated lasers [23]. On another note, the 6-dB extinction ratio is a common value in systems employing vertical cavity surface emitting laser sources [24]. It is noteworthy that analytical results were verified by Monte Carlo simulations showing a perfect agreement. Hence, and for the sake of clarity, they are not plotted here.

As we can see, the lower the extinction ratio, the poorer behavior in terms of BER. Accordingly, the behavior is also deteriorated when the turbulence regime is more severe. It is also interesting to notice that the weaker the turbulence intensity, the smaller the difference between the curves corresponding to ideal extinction ratio and to an extinction ratio of 11 dB. Conversely, the difference in average BER between the case of an extinction ratio of 11 dB and an extinction ratio of 6 dB is more pronounced for a weaker turbulence than for a stronger turbulence. For instance, for an average BER of 10^{-5} and $\sigma_I^2 = 0.061$, there exists a difference of 0.72 dB between the curves associated to the ideal case of an infinite extinction ratio with respect to the curve with an extinction ratio of 11 dB; and this difference is increased up to 4.09 dB when comparing the curve associated to an extinction ratio of 6 dB with respect to the one with an extinction ratio of 11 dB. However, these differences are, respectively 3.48 and

1.98 dB for a turbulence regime of $\sigma_I^2 = 3$. The reason is that turbulence is becoming the dominant source of degradation when turbulence strength is higher.

7. Concluding remarks

In this paper, we have presented new different features involving the Málaga generalized statistical model. First we have analyzed the performance of an IM/DD optical system employing an OOK scheme when the detection threshold is fixed. In that case, the system is unable to adapt itself to the varying conditions of the channel and a limit in terms of error floor is obtained. In particular, the analytical closed-form expression for that error rate was derived in this paper for different turbulent regimes, showing that its intensity, in terms of σ_I^2, is the parameter that finally determines the value of the error floor. Hence, the less intense the turbulent process is, the lower error floor is reached in terms of BER.

After that, we have examined a situation where the system does not have a perfect knowledge of the instantaneous CSI. Nevertheless, it can be assumed that the turbulent process is considered, not as a local stationary random process, but with stationary increments. Thus, its mean and variance can be known assuming that the atmospheric turbulence is a slow random process in comparison with the typical data rates employed in these optical links. Therefore, the system can monitor these two statistical moments without a penalization in the effective data rate. Accordingly, we have derived some expressions to obtain the optimal threshold detection from a likelihood function. We have distinguished two different scenarios: a first one, ideal, without being affected by the finite extinction ratio; and a second scenario in which we consider a non-ideal laser operating in the system, and characterized by transmitting a small amount of power even when a logic bit 0 is sent. We have selected realistic values for this extinction ratio corresponding to different commercially available lasers as, for example, the vertical cavity surface emitting laser source or the Mach–Zehnder one. We have shown that the effect of a non-negligible reduction of the extinction ratio causes an increment in the value of the required optimal threshold in an adaptive system. This behavior is quite logical since those non-ideal lasers introduce a type of offset in the power they issue.

A further step was presented in Section 6. There, it was assumed that the CSI was perfectly known by the optical system taking advantage, once again, of the fact that the atmospheric turbulence behaves as a slow process and it will not change significantly during a finite observation time. Thus, it is feasible to monitor the real CSI with the transmission of some pilot signals every atmospheric turbulence correlation time τ_0. To support that assumption, this τ_0 is again supposed to be much larger than the bit period. The benefit is straightforward: analytical expressions for the BER of an adaptive system can be derived for the generic case of realistic lasers characterized by any particular offset ζ. It is shown that the larger this ζ parameter becomes (or the smaller the extinction ratio is), the worse performance in terms of BER we obtain. For stronger turbulence regimes, however, the turbulence intensity constitutes the dominant factor

of degradation in the system. Consequently, the relevant parameters limiting the behavior of a system are: the turbulence intensity, the amount of additive white Gaussian noise and the value of the extinction ratio associated to a laser and available in its specification sheet.

Finally, it is possible to introduce the adverse effect of a potential ISI when the assumption of having a sufficient bandwidth in the receiver filter is not accomplished [14]. For that situation, the starting point will be the expression of BER derived by KAHN *et al*. (Eqs. (9) and (10) in [15]) that should be considered as a conditional error probability and, in this respect, it must be subsequently averaged over the PDF of the Málaga distribution. Hence, the resulting average BER becomes a deteriorated and shifted version of the ones obtained in this paper for the ideal case of not having considered ISI in the system.

Acknowledgements – This work was supported by the Andalucía Talent Hub Program launched by the Andalusian Knowledge Agency, co-funded by the European Union's Seventh Framework Program, Marie Skłodowska-Curie actions (COFUND – Grant Agreement No. 291780) and the Ministry of Economy, Innovation, Science and Employment of the Junta de Andalucía; and by the Spanish Ministerio de Economía y Competitividad, Project TEC2012-36737.

References

[1] ANDREWS L.C., PHILLIPS R.L., *Laser Beam Scintillation through Random Media*, 2nd Ed., SPIE, 2005.

[2] KAZAURA K., WAKAMORI K., MATSUMOTO M., HIGASHINO T., TSUKAMOTO K., KOMAKI S., *RoFSO: a universal platform for convergence of fiber and free-space optical communication networks*, IEEE Communications Magazine **48**(2), 2010, pp. 130–137.

[3] JURADO-NAVAS A., GARRIDO-BALSELLS J.M., CASTILLO-VÁZQUEZ M., PUERTA-NOTARIO A., *An efficient rate-adaptive transmission technique using shortened pulses for atmospheric optical communications*, Optics Express **18**(16), 2010, pp. 17346–17363.

[4] VEGAS OLMOS J.J., PANG X., LEBEDEV A., SALES LLOPIS M., TAFUR MONROY I., *Wireless and wireline service convergence in next generation optical access networks – the FP7 WISCON project*, IEICE Transactions on Communications **E97-B**(8), 2014, pp. 1537–1546.

[5] JURADO-NAVAS A., TATARCZAK A., XIAOFENG LU, VEGAS OLMOS J.J., GARRIDO-BALSELLS J.M., TAFUR MONROY I., *850-nm hybrid fiber/free-space optical communications using orbital angular momentum modes*, Optics Express **23**(26), 2015, pp. 33721–33732

[6] AL-HABASH M.A., ADREWS L.C., PHILLIPS R.L., *Mathematical model for the irradiance probability density function of a laser beam propagating through turbulent media*, Optical Engineering **40**(8), 2001, pp. 1554–1562.

[7] JURADO-NAVAS A., GARRIDO-BALSELLS J.M., PARIS J.F., PUERTA-NOTARIO A., *A unifying statistical model for atmospheric optical scintillation*, [In] *Numerical Simulations of Physical and Engineering Processes*, [Ed.] Awrejcewicz J., In-Tech, 2011, pp. 181–206.

[8] GARRIDO-BALSELLS J.M., JURADO-NAVAS A., PARIS J.F. CASTILLO-VÁZQUEZ M., PUERTA-NOTARIO A., *General analytical expressions for the bit error rate of atmospheric optical communicatino systems: erratum*, Optics Letters **39**(20), 2014, pp. 5896–5896.

[9] JURADO-NAVAS A., GARRIDO-BALSELLS J.M., CASTILLO-VÁZQUEZ M., PUERTA-NOTARIO A., *Closed -form expressions for the lower-bound performance of variable weight multiple pulse-position modulation optical links through turbulent atmospheric channels*, IET Communications **6**(4), 2012, pp. 390–397.

[10] JURADO-NAVAS A., GARRIDO-BALSELLS J.M., CASTILLO-VÁZQUEZ M., PUERTA-NOTARIO A., *Numerical model for the temporal broadening of optical pulses propagating through weak atmospheric turbulence*, Optics Letters **34**(23), 2009, pp. 3662–3664.

[11] YOUNG C.Y., ANDREWS L.C., ISHIMARU A., *Time-of-arrival fluctuations of a space–time Gaussian pulse in weak optical turbulence: an analytic solution*, Applied Optics **37**(33), 1998, pp. 7655–7660.

[12] XIAOMING ZHU, KAHN J.M., *Free-space optical communication through atmospheric turbulence channels*, IEEE Transactions on Communications **50**(8), 2002, pp. 1293–1300.

[13] JURADO-NAVAS A., GARRIDO-BALSELLS J.M., CASTILLO-VÁZQUEZ M., PUERTA-NOTARIO A., *A computationally efficient numerical simulation for generating atmospheric optical scintillations*, [In] *Numerical Simulations of Physical and Engineering Processes*, [Ed.] Awrejcewicz J., In-Tech, 2011, pp. 157–180.

[14] GARCIA-ZAMBRANA A. PUERTA-NOTARIO A., *Improving PPM schemes in wireless infrared links at high bit rates*, IEEE Communications Letters **5**(3), 2001, pp. 95–97.

[15] KAHN J.M., KRAUSE W.J., CARRUTHERS J.B., *Experimental characterization of non-directed indoor infrared channels*, IEEE Transactions on Communications **43**(2/3/4), 1995, pp. 1613–1623.

[16] AHARONOVICH M., ARNON S., *Performance improvement of optical wireless communication through fog with a decision feedback equalizer*, Journal of the Optical Society of America A **22**(8), 2005, pp. 1646–1654.

[17] GRADSHTEYN I.S., RYZHIK I.M., *Table of Integrals, Series and Products*, 7th Ed., Academic Press, New York, 2007.

[18] XIAOMING ZHU, KAHN J.M., *Pilot-symbol assisted modulation for correlated turbulent free-space optical channels*, Proceedings of SPIE **4489**, 2002, pp. 138–145.

[19] MORADI H., REFAI H.H., LOPRESTI P.G., *Thresholding-based optimal detetion of wireless optical signals*, Journal of Optical Communications and Networking **2**(9), 2010, pp. 689–700.

[20] Wolfram, http://functions.wolfram.com

[21] ANSARI I.S., AL-AHMADI S., YILMAZ F., ALOUINI M.S., YANIKOMEROGLU H., *A new formula for the BER of binary modulations with dual-branch selection over generalized-K composite fading channels*, IEEE Transactions on Communications **59**(10), 2011, pp. 2654–2658.

[22] KIUCHI H., KAWANISHI T., YAMADA M., SAKAMOTO T., TSUCHIYA M., AMAGAI J., IZUTSU M., *High extinction ratio Mach–Zehnder modulator applied to a highly stable optical signal generator*, IEEE Transactions on Microwave Theory and Techniques **55**(9), 2007, pp. 1964–1972.

[23] SUHR L.F., VEGAS OLMOS J.J., MAO B., XU X., LIU G.N., TAFUR MONROY I., *112-Gbit/s × 4-lane duobinary-4-PAM for 400GBase*, [In] *2014 The European Conference on Optical Communication (ECOC)*, 2014, pp. 1–3.

[24] PRINCE K., MING MA, GIBBON T., NEUMEYR C., RÖNNEBERG E., ORTSIEFER M., MONROY I.T., *Free -running 1550 nm VCSEL for 10.7 Gb/s transmission in 99.7 km PON*, IEEE/OSA Journal of Optical Communications and Networking **3**(5), 2011, pp. 399–403.

Received February 26, 2016
in revised form April 20, 2016